Yamartino, R., 2010. *Special Applications of Gaussian Models*. Chapter 9 of *AIR QUALITY MODELING - Theories, Methodologies, Computational Techniques, and Available Databases and Software. Vol. IV – Advances and Updates* (P. Zannetti, Editor). Published by The EnviroComp Institute (www.envirocomp.org) and the Air & Waste Management Association (www.awma.org).

Chapter 9

Special Applications of Gaussian Models

Robert J. Yamartino

Integrals Unlimited, Portland, Maine (*USA*)
rjy@maine.rr.com

Abstract: This chapter focuses first on the mathematical fundamentals of the Gaussian distribution that bear on its applicability to air quality modeling. These fundamental properties include: that any weighted sum of Gaussian PDFs is itself a Gaussian PDF; that the Fourier transform of a Gaussian is itself a Gaussian; and, that the convolution of a Gaussian with a Gaussian results in a Gaussian. The impact of these fundamentals includes: the connection between the Gaussian velocity PDF and the Gaussian shape of the concentration distribution; the ability to generate mean plumes from an instantaneous plume and a meander envelope; the ability to compute higher-order concentration statistics; and the ability to compute non-linear chemical reactions. Finally, some recent changes to U.S. EPA regulatory Gaussian models are considered.

Key Words: Gaussian methods, atmospheric dispersion modeling.

Given the previous three chapters (i.e., 7A by Venkatram and Thé, 2003, and 7B and 8A by Yamartino, 2008a-b) devoted to Gaussian plume and puff modeling that have appeared in this series, the challenge of this chapter is to avoid repetition and cover areas of application interest that have yet to be covered. While the emphasis will be on applications, one cannot help but first look at some mathematical fundamentals of the Gaussian distribution that bear on its applicability to air quality modeling. The focus will then shift to more specific applications of the Gaussian formulation to air pollution problems and finally to more recent issues with Gaussian-based regulatory models.

1 Some Mathematical Properties of the Gaussian and Their Practical Implications

While the choice of the Gaussian for analytic air pollution modeling applications may seem to have been a somewhat arbitrary choice among suitably peaked and appropriately normalized functions, there are additional mathematical properties of the Gaussian that have proven to be quite advantageous. These fundamental properties include the facts that:

- Any weighted sum of Gaussian probability distribution functions (PDFs) is itself a Gaussian PDF;
- The Fourier transform of a Gaussian is itself a Gaussian; and,
- The convolution of a Gaussian with a Gaussian results in a Gaussian.

It should also be noted that the Gaussian is singled out by the Central Limit Theorem as it states that the mean of a large number of independent random variables, each with finite mean and variance but possessing arbitrary though identical distributional properties, will converge toward being approximately normally distributed.

1.1 Gaussian PDFs Connecting Velocity and Spatial Distribution PDFs

The mathematical property that any weighted sum of Gaussian PDFs is itself a Gaussian PDF can be expressed as:

$$\sum_{i=1}^{n} \mathrm{a}_i \cdot N_i(\mu_i, \sigma_i) = b \cdot N\left(\sum_{i=1}^{n} (\mathrm{a}_i \cdot \mu_i) \, , \sqrt{\sum_{i=1}^{n} (\mathrm{a}_i \cdot \sigma_i)^2} \right) \tag{1}$$

where $N(\mu, \sigma)$ represents a Normal (i.e., or Gaussian) PDF having a mean of μ and a standard deviation of σ, a_i are scalar multipliers, and where b is a multiplier that provides the proper normalization of the composite PDF. Its proof can most easily be found in Lemons (2002, Chapter 2) or online at: http://en.wikipedia.org/wiki/Sum_of_normally_distributed_random_variables.

This relationship bears on issues such as why Gaussian turbulent velocity distributions are consistent with Gaussian concentration profiles for a point source and why the Gaussian plume/puff solutions permit miniscule concentrations to exist at great distances from a source even just after release.

Consider first the question of why the Gaussian analytic solution to the diffusion equation allows diffused mass to exist at infinite distances from the source in apparent defiance of any reasonable causal linkage. If one instead begins with a Gaussian turbulent velocity distribution, Lemons (2002, Chapter 7) has shown that within the framework of a Langevin stochastic equation for homogeneous flow, the turbulent velocity PDF will always remain Gaussian with a mean of zero and a variance of σ_v^2. This is because for homogeneous turbulence (i.e., no

turbulence gradient in the dimension of interest), the Langevin equation updates individual particle turbulent velocities via the relation:

$$v(n\cdot\Delta t) = v[(n\text{-}1)\cdot\Delta t]\cdot f + \sigma_v\cdot(1 - f^2)^{1/2}\cdot R(0,1)\ , \qquad (2)$$

where $R(0,1)$ is a random Gaussian number having a mean of zero and a standard deviation of unity, $f = \exp(-\Delta t/\tau)$, and τ is the Lagrangian time scale. Equation (1) then guarantees that this turbulent velocity PDF will remain normal with constant variance, as $f^2 + (1 - f^2)$ just equals one. As the corresponding particle position, $y(t)$, is computed as a sum over these velocities for various time steps multiplied by the scalar Δt, Equation (1) again provides the guarantee that this distribution of particle positions will remain normal. Durbin (1983), Van Dop et al. (1985), and others have shown that the resulting variance of this normal PDF of particle positions is:

$$\sigma_y^2 = 2\cdot\sigma_v^2\cdot\tau^2\cdot[\ t/\tau + \exp(-t/\tau) - 1]\ , \qquad (3)$$

which for early times (i.e., $t << \tau$) provides for a linear-in-time growth of σ_y as $\sigma_y = \sigma_v\cdot t$, and, for late times (i.e., $t >> \tau$) a $t^{1/2}$ growth as $\sigma_y = 2^{1/2}\cdot\sigma_v\cdot(t\cdot\tau)^{1/2}$. This late time result is consistent with the K-theory solution with $K_y = \sigma_v^2\cdot\tau$.

Regardless of the initial shape of the turbulent velocity PDF, Pope (2000) has shown that the diffusion term in the underlying differential equation governing the evolution of the turbulent velocity PDF will make it tend towards normal asymptotically. Further, the assumption of a Gaussian PDF for turbulent velocities has been shown by Wilson (2007) to provide a superior fit to Prairie Grass data than three other PDF distributions having attenuated (e.g., $\exp[-v^4/(\gamma\cdot\sigma_v^4)]$, with γ as a fitting constant) or no (e.g., triangular or cosine PDF) high-velocity, v, tails extending out to infinity.

Thus, returning to the Gaussian profile function, $\exp[-y^2/(2\cdot\sigma_y^2)]$, any concern we might have had over the minute amounts of material at large crosswind distance, y, should now be soothed by knowledge that the corresponding Gaussian turbulent velocity distribution implies a similarly minute amount of material "diffusing" outward at extremely high transverse velocities. Were one to find a well-behaved and superior PDF functional form with such high velocity tails "clipped" away from the distribution, then that would provide a basis for beginning anew; however, the effort involved would likely not prove to be worthwhile, especially now that one understands the relatively benign source of this material found at unlikely transverse distances of many, many σ_y. In the vertical direction, the presence of a gradient in turbulence leads to a skewed velocity PDF, particularly in the case of convective conditions (Luhar and Britter, 1989). One notes that a skewed Gaussian PDF, with its mean shifted by an appropriate area weighted average of updraft and downdraft velocities, can generally accommodate such situations.

1.2 Fourier Transform of a Gaussian is a Gaussian

The Gaussian distribution is also the only functional form for which its Fourier transform is also a Gaussian. To understand this solution characteristic better, we note that the process of taking the Fourier transform of the Gaussian in space (i.e., by multiplying the Gaussian profile shape times the quantity $exp(-i \cdot k \cdot x)$, where i is the imaginary number, and integrating over all x from $-\infty$ to $+\infty$) yields a Gaussian distribution in k, the conjugate variable to x. Now k, with its units that must be in terms of inverse distance is often referred to as wavenumber, and is usually defined in terms of wavelength as $k \equiv 2 \cdot \pi / \lambda$. Another curious property of this Fourier-transform k-space distribution is that this Gaussian distribution, centered at k=0, has a standard deviation inversely proportional to the standard deviation of the original x distribution of the Gaussian solution. More explicitly, one finds that:

$$\sigma_x \cdot \sigma_k = \tfrac{1}{2} . \tag{4a}$$

One notes that beginning with any other, non-Gaussian distributions results in a different non-Gaussian distribution for the transformed variable, and the subsidiary finding for non-Gaussians that:

$$\sigma_x \cdot \sigma_k > \tfrac{1}{2} . \tag{4b}$$

Those familiar with quantum mechanics will recall that this mathematical relationship between conjugate variables looks a bit like the Heisenberg Uncertainty Principal. In fact, all we have to do to get there is first recall that at the quantum level, a particle's momentum, p, is simply its wavenumber times the reduced Plank constant, $\hbar \equiv h / (2 \cdot \pi)$, then one obtains the Heisenberg result of:

$$\sigma_x \cdot \sigma_p \geq \hbar / 2 \text{ , or } \Delta x \cdot \Delta p \geq \hbar / 2 \tag{4c}$$

in the more conventional physics notation. Of course, the interpretation of this relation in the Heisenberg Uncertainty Principal case is quite different than the one we consider here, but the Fourier Transform mathematical basis is the same in both cases.

Further analysis of the Gaussian distribution in k-space shows that as the spatial distribution grows, energy is fed into the shorter k values (i.e., $k \cdot \sigma_y < 0.5$) and depleted from k values for which $k \cdot \sigma_y > 0.5$. This increase in the long wave portion (i.e., $\lambda > 4 \cdot \pi \cdot \sigma_y$) indicates that classical diffusion is a smoothing process that would tend to wipe out concentration fluctuations with plume growth. Thus, it is not surprising that the Gaussian plume formulation is considered most appropriate for time-averaged or ensemble-averaged concentration measures.

1.3 Convolution of Gaussians Yields a Gaussian

Another interesting property of the Gaussian is that the convolution of a Gaussian with a Gaussian results in a Gaussian. This property has the important consequence that one can now envision splitting the turbulent velocity spectra into a short-wave component leading to the physical plume's spreading and a long-wave component that causes the entire plume to meander back and forth. While such a division may seem overly-simplistic, it has served as the basis for meandering plume models which represent one of the earliest attempts (e.g., Gifford, 1959) to model concentration fluctuations. The convolution process is defined mathematically as:

$$Y(y,\sigma_T) \equiv \{P,\phi\} \equiv \int_{-\infty}^{+\infty} dy' \cdot P(y-y',\sigma_p) \cdot \phi(y',\sigma_m) \ , \tag{5}$$

where the instantaneous plume is given as:

$$P(y-y',\sigma_p) = \frac{1}{\sqrt{2\pi}\cdot\sigma_p} \cdot \exp\left[-\frac{(y-y')^2}{2\cdot{\sigma_p}^2}\right] \tag{6a}$$

and $\sigma_p = \sigma_p(t)$ characterizes the width of the instantaneous plume and the presumed Gaussian envelope defining the plume's meander is given as:

$$\phi(y,\sigma_m) = \frac{1}{\sqrt{2\pi}\cdot\sigma_m} \cdot \exp\left[-\frac{y'^2}{2\cdot{\sigma_m}^2}\right] \tag{6b}$$

The result of performing this convolution integration yields a normalized Gaussian distribution, $Y(y,\sigma_T)$,

$$Y(y,\sigma_T) = \frac{1}{\sqrt{2\pi}\cdot\sigma_T} \cdot \exp\left[-\frac{y'^2}{2\cdot{\sigma_T}^2}\right] \tag{7a}$$

with

$${\sigma_T}^2 = {\sigma_p}^2 + {\sigma_m}^2 \ . \tag{7b}$$

Performing the integral in Equation (5) requires little more than the technique of "completing the square". Knowing this, it is clear that the process of performing the Equation (5) integration yields a multiplicative factor, β, [1]

---

[1] Obtaining the correct factor requires knowing that $M \equiv \int_{-\infty}^{+\infty} dx \cdot \exp\left[-x^2\right] = \sqrt{\pi}$; however, this is computed by solving for M^2 and then shifting to (r,θ) coordinates.

where $$\beta = \frac{\sqrt{2\pi} \cdot \sigma_m \cdot \sigma_p}{\sigma_T} \quad . \tag{7c}$$

Implicit in the convolution process is the assumption that the processes of plume growth and plume meander are independent of one another. This independence may also be apparent from the quadrature addition rule for sigmas resulting in the total plume width, σ_T.

Those familiar with the Convolution or Faltung Theorem, which states that:

$$F(\{P,\varphi\}) = k \cdot F(P) \cdot F(\varphi) \; . \tag{8}$$

where F denotes the Fourier transform process and k is a normalization constant, will note that the idea that the convolution of two Gaussians results in a Gaussian is obvious given the above Convolution Theorem and the fact that the Fourier transform of a Gaussian is a Gaussian.

Thus, beyond the Gaussian representing the simplest K-theory solution to the diffusion equation, there are many mathematical conveniences to be had by choosing the Gaussian, and also there are clear physically-significant linkages (e.g., between observed Gaussian turbulent velocity distributions and the Gaussian concentration profiles obtained from the analytic solution for diffusion) and statistical properties (e.g., the independence of turbulent components of widely different wavelengths) that make the Gaussian the logical distribution of choice for puff and plume modeling.

2 Gaussian Applications

This section will consider applications involving the Gaussian or the Gaussian solution of the diffusion equation, which greatly facilitate obtaining additional results.

2.1 Concentration Fluctuations

As mentioned above, the convolution of an instantaneous Gaussian plume having a spread σ_p with a Gaussian meander envelope of spread σ_m leads to an ensemble-averaged Gaussian plume of width σ_T , where $\sigma_T^2 = \sigma_m^2 + \sigma_p^2$, such that peak-to-mean centerline concentrations are just σ_T / σ_p .

First developed by Gifford (1959) and extended by others, including Hanna (1986) and Sawford and Stapountzis (1986), Equation (5) may be integrated and generalized to yield higher moments of the concentration distribution as:

$$Y^{(n)}(y,\sigma_{Tn}) = \int_{-\infty}^{+\infty} dy' \cdot P^n(y-y',\sigma_p) \cdot \phi(y',\sigma_m) \ . \tag{9a}$$

By analogy with the Equation (5) integration, we note that performing the Equation (9a) integration will yield the exponential's multiplier, β_n,

where

$$\beta n = \frac{\sqrt{2\pi} \cdot \sigma_m \cdot \sigma_p}{\sigma_{Tn} \cdot \sqrt{n}} \tag{9b}$$

and where

$$\sigma_{Tn}{}^2 = \sigma_m{}^2 + \sigma_p{}^2/n \ . \tag{9c}$$

Thus, $Y^{(2)}$ has centerline (i.e., $y = 0$) value

$$Y^{(2)}(0,\sigma_{T2}) = \frac{1}{\sqrt{2\pi} \cdot \sigma_m \cdot 2\pi \cdot \sigma_p^2} \cdot \beta 2 = \frac{1}{2\pi \cdot \sqrt{2} \cdot \sigma_p \cdot \sigma_{T2}} \tag{10a}$$

with

$$\sigma_{T2}{}^2 = \sigma_m{}^2 + ½ \cdot \sigma_p{}^2 \ ; \tag{10b}$$

whereas,

$$Y^{(1)}(0,\sigma_{T1}) = \frac{1}{\sqrt{2\pi} \cdot \sigma_{T1}} \quad , \tag{11a}$$

with

$$\sigma_{T1}{}^2 = \sigma_m{}^2 + \ \sigma_p{}^2 \ . \tag{11b}$$

One may then compute the concentration variance, $\sigma_C{}^2$, as $\sigma_C{}^2 \equiv Y^{(2)}$ - $(Y^{(1)})^2$ or that variance normalized by the mean concentration squared as,

$$\frac{\sigma_C^2}{\left(Y^{(1)}\right)^2} = \left[\frac{\sigma_{T1}^2}{\sqrt{2} \cdot \sigma_p \cdot \sigma_{T2}} \text{ -1} \right] \tag{12}$$

Of course, this concentration variance only reflects plume fluctuations due to meander in y, as $\sigma_C \rightarrow 0$ as $\sigma_m \rightarrow 0$, and ignores any variations in the z direction. It also ignores concentration fluctuations internal to the narrow plume of width σ_p;

however, now we are beginning to delve into the well-developed specialty of concentration fluctuations, which would require a chapter of its own. The point here was to show the flexibility of the Gaussian and the ease to which one can obtain meaningful results by invoking the convolution theorem.

2.2 Diffusion into Soils

Deposition rates of air pollutants is predicted by a number of regulatory models worldwide, and the results of these surface deposition predictions are then used by other disciplines (e.g., soil scientists interested in watershed acidification, toxicologists assessing lead concentrations in surface soils), but the applications can go much deeper than that -- quite literally. For example, long-lived radioactive isotopes, such as ^{137}Cs deposited over many European countries during the 1986 Chernobyl incident continue to "diffuse" their way deeper into the soils and are readily detectable in core samples (e.g., Rosen et al., 1999; Doering et al., 2006; Kaste et al., 2007).

From Chapter 7B, Vol. 2 of Zannetti (2005), we know that the 1-d time-dependent solution of the diffusion equation is:

$$\phi(y,\sigma) = \frac{1}{2 \cdot \sqrt{\pi \cdot K \cdot t}} \cdot \exp\left[-\frac{z^2}{4 \cdot K \cdot t} \right], \tag{13}$$

where K is now the diffusivity of the soil, with values typically in the range of one cm^2/yr or less (i.e., some 12 orders of magnitude smaller than the rather stable atmospheric diffusivity of 3 m^2/s), and z is assumed positive in the direction downward into the soil. Carslaw and Jaeger (1959) showed that for a constant surface deposition rate, Q (g/cm^2/yr), to the surface (i.e., $z=0$) for all $t \geq 0$, the solution for soil concentration, C_S (gm/cm^3) as a function of depth and time is:

$$C_s(z,t) = \frac{Q}{K}\left[\sqrt{\frac{K \cdot t}{\pi}} \exp\left(\frac{-z^2}{4 \cdot K \cdot t} \right) - \frac{z}{2} erfc\left(\frac{z}{2 \cdot \sqrt{K \cdot t}} \right) \right] \tag{14}$$

where, as before, *erfc(x)* is the complementary error function, *erfc(x)* ≡ 1 – *erf(x)*, and any diffusion upward into the atmosphere is prohibited (i.e., thus accounting for a factor-of-two multiplier) as are all other loss or decay mechanisms. Under such conditions, soil concentrations always increase with total time of deposition.

Now in the more realistic case, deposition occurs up to some cutoff time, $t' = T$, such that for observation times $t > T$, only additional diffusion occurs. Interestingly, there are several ways to formulate this problem. The first is to take the distribution from Equation (14) at time $t = T$ and allow it to diffuse for times $t > T$ via:

$$C_s(z,t)=\left(\frac{2\cdot Q}{K}\right)\cdot\int_0^{\infty}dz'\cdot\frac{\left[\sqrt{\frac{K\cdot T}{\pi}}\exp\left(\frac{-z'^2}{4\cdot K\cdot T}\right)-\frac{z'}{2}erfc\left(\frac{z'}{2\sqrt{K\cdot T}}\right)\right]}{\sqrt{\pi\cdot K\cdot(t-T)}}\cdot\exp\left(\frac{-(z-z')^2}{4\cdot K\cdot(t-T)}\right) \quad (15a)$$

however, the part of this integral involving the convolution of the *erfc* with the Gaussian appears rather difficult to solve. Alternatively, one could back up a step from Equation (14) and express the problem as the double-integral:

$$C_s(z,t)=2\cdot Q\cdot\int_0^{\infty}dz'\cdot\int_0^{T}dt'\cdot\frac{\exp\left(\frac{-z'^2}{4\cdot K\cdot t'}\right)}{\sqrt{4\cdot\pi\cdot K\cdot t'}}\cdot\frac{\exp\left(\frac{-(z-z')^2}{4\cdot K\cdot(t-T)}\right)}{\sqrt{4\cdot\pi\cdot K\cdot(t-T)}}\ . \quad (15b)$$

Note that in this expression, the √4 constant factors have been left in place to show that the overall factor of 2 is needed to account for material at the surface not diffusing upward into the air, but being "reflected" back into the soil. One may then solve this problem by reversing the order of the integrations and performing the spatial convolution first; however, this approach is equivalent to the more direct approach of specifying the diffusion of an emission $Q\cdot dt'$ for all $t > t'$ and then integrating over time t' to yield the concentrations at a specific depth z for $t > T$ as:

$$C_s(z,t)=2\cdot\int_0^{T}\frac{dt'\cdot Q(t')}{\sqrt{4\cdot\pi\cdot K\cdot(t-t')}}\exp\left(\frac{-z^2}{4\cdot K\cdot(t-t')}\right)\ ; \quad (15c)$$

whereas, the concentration averaged over a depth interval $L\equiv z_2 - z_1$, (i.e., from depth z_1 to depth z_2) can then be written as:

$$C_{s,ave}(t)=\frac{1}{L}\cdot\int_0^{T}dt'\cdot Q(t')\cdot\left\{erf\left(\frac{z_2}{2\cdot\sqrt{K\cdot(t-t')}}\right)-erf\left(\frac{z_1}{2\cdot\sqrt{K\cdot(t-t')}}\right)\right\} \quad (16)$$

Drivas et al. (2010) have shown that these last two integrals can be solved by changing from variable t' to s, where $s=\frac{\lambda}{2\cdot\sqrt{K\cdot(t-t')}}$, $dt'=\left(\frac{\lambda^2}{2\cdot K}\right)\cdot\frac{ds}{s^3}$, and, where λ stands for either z, z_2 or z_1. Their final results for $t > T$ are found to be:

$$C_s(z,t)=\frac{Q\cdot z}{K}\cdot\left[f(s_L)-f(s_U)\right]\ , \quad (17)$$

where $f(s) \equiv \left[\frac{\exp\left(-s^2\right)}{\sqrt{\pi} \cdot s} + erf(s) \right]$, $s_L = \frac{z}{2\sqrt{K \cdot t}}$ and $s_U = \frac{z}{2\sqrt{K \cdot (t-T)}}$; and,

$$C_{s,ave}(t) = \frac{Q \cdot L^{-1}}{2 \cdot K} \cdot \left\{ z_2^2 \cdot \left[g\left(s_{L2}\right) - g\left(s_{U2}\right) \right] - z_1^2 \cdot \left[g\left(s_{L1}\right) - g\left(s_{U1}\right) \right] \right\} \tag{18}$$

where $g(s) \equiv \left[\frac{\exp\left(-s^2\right)}{\sqrt{\pi} \cdot s} + \left(1 + \frac{1}{2 \cdot s^2}\right) \cdot erf(s) \right]$, $s_{L2} = \frac{z_2}{2\sqrt{K \cdot t}}$, $s_{U2} = \frac{z_2}{2\sqrt{K \cdot (t-T)}}$,

$s_{L1} = \frac{z_1}{2\sqrt{K \cdot t}}$ and $s_{U1} = \frac{z_1}{2\sqrt{K \cdot (t-T)}}$.

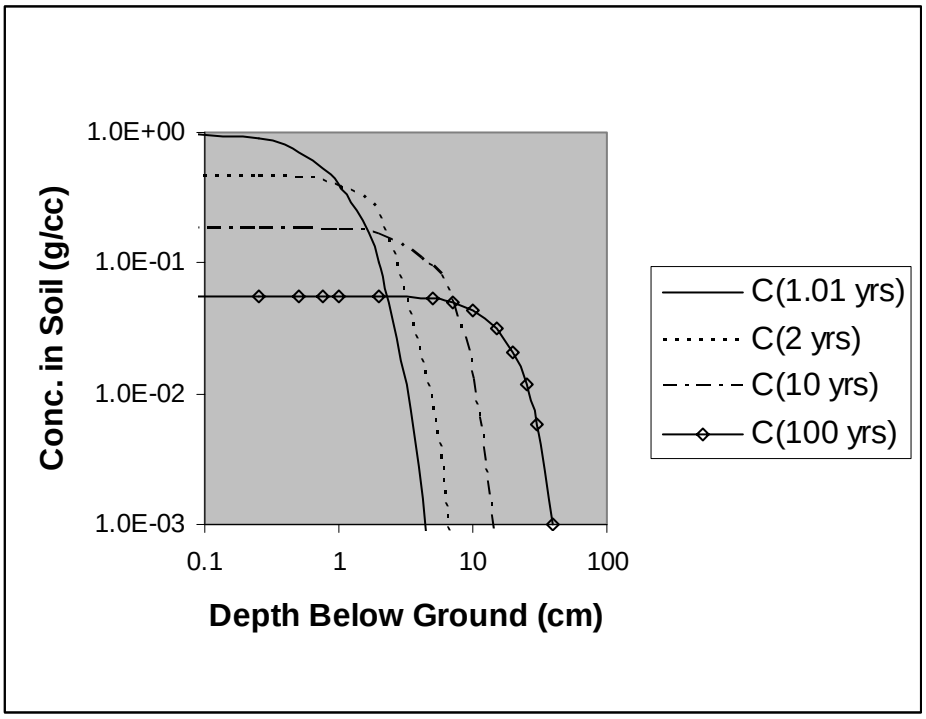

Figure 1. Equation (17) concentrations in soil vs. depth below surface at various times for a unit strength deposition, Q=1 g/m^2/yr, beginning at t=0 and having a duration of T = 1 yr. A unit diffusivity of K=1.0 cm^2/yr is also assumed.

Evaluation of these expressions, such as the Equation (17) curves displayed above, show that radioactive, or other non-reactive, species concentrations can show up at some depth, well below the surface, decades after at the deposition at the surface has ceased. This insidious march of hazardous pollutants to deeper depths and eventually to groundwater levels has been the driving force behind many Superfund projects, including the massive cleanup effort in Hanford, WA,

site of many nuclear research activities from the mid-1940s through the late 1980s. Thus, one sees that new and relevant applications of purely Gaussian-based solution formulations continue to be developed and applied.

2.3 Non-Linear Chemistry in Puff Modeling

Photochemical grid models now constitute the major vehicle for addressing ozone and secondary particulate impact issues; however, pure grid models suffer from the shortcoming that point-source emissions are immediately diluted into a grid-cell-sized box of dimensions $dx \cdot dy \cdot dz$. This initial instantaneous dilution ignores near-source, within-plume conversion processes, which can occur very rapidly given the high-concentrations of primary pollutants near the source.

One approach to dealing with this problem is to employ a nested-grid approach, and this approach is often used in regional modeling with horizontal resolutions over source-rich urban or industrial source areas nested down to about 1 km. Nevertheless, initial dilution into a box that is one kilometer squared in area leaves much early chemistry neglected. This early chemistry is now tackled by using various types plume-in-grid (PiG) modules to facilitate reaction of the pollutants close to the source and transport them until the plume's or puff's size is comparable to the grid resolution, whereupon the material is injected into the grid model itself.

Early PiG models involved Gaussian plumes, but it was quickly realized that one needed yet higher, sub-plume scale resolution, so there was a pronounced shift towards using puffs instead. Of course, once starts to think in terms of puffs, the transition to very small puffs or even Lagrangian particles having some finite spatial extent is more a leap of computational intensity than a conceptual one.

To understand the basic challenge of performing non-linear chemistry using puffs, we begin with the basic equation for chemical transformations within an N-species system. In general, the set of N equations describing the time evolution of species mixing ratios[2], $c(t)_i$, that undergo 1st, 2nd, and pseudo-3rd order chemical reactions can be written as:

$$\frac{dc_i(\mathrm{t})}{d\,\mathrm{t}} = \sum_{j=1}^{N} \sum_{k=j}^{N} \mathrm{R}_{\mathrm{i}}^{\mathrm{jk}} \cdot \mathrm{c}_j(\mathrm{t}) \cdot \mathrm{c}_k(\mathrm{t}) \,, \quad \mathrm{i, j, k} = 1,2,3,..., \mathrm{N} \,, \tag{19}$$

where R_i^{jk} is the matrix (i.e., rank-3 tensor) of chemical reaction rates. Now invoking the convention of implied summation over repeated indices (i.e., j and k) and integrating over some agree-upon volume of space one has the equation system:

[2] A mass concentration, C_i , relates to the dimensionless mixing ratio, c_i via the relation $C_i = \rho \cdot c_i$.

$$\frac{dm_i(\mathrm{t})}{d\,\mathrm{t}} = \iiint_V \rho \cdot \frac{dc_i(\mathrm{t})}{d\,\mathrm{t}} = \mathrm{R}_{\mathrm{i}}^{\mathrm{jk}} \cdot \iiint_V \rho \cdot \mathrm{c}_j(\mathrm{t}) \cdot \mathrm{c}_k(\mathrm{t}) \,, \quad \mathrm{i, j, k} = 1,2,3,..., \mathrm{N} \,, \qquad (20)$$

where ρ is the local air density. In the case of grid modeling, the volume, V, to be integrated over is simply the volume of the current cell being considered, and within-cell mixing ratios and masses are related simply by, $m_i = \rho \cdot c_i \cdot V$. However, in the case of dealing with puffs or particles, we have the additional complications that concentrations of each species at any single point can involve the summation over many nearby puffs and that the volumes to be associated with each particle or puff will definitely overlap those volumes associated with other particles or puffs.

Thus, even the definition of species mixing ratios c_i, c_j, and c_k at any point involve sums over all puffs that could possibly contribute to species concentrations at that point. Because any product of sums can always be re-expressed of a sum of products, one sees that the computation of species concentrations involves the spatially-integrated product of the spatial distributions associated with some puff p and any other puff m. Choice of the indices p and m was done partly to avoid confusion with the already used pollutant species indices i, j, and k but also to facilitate bridging back to Equation (5) where our interest was in integrating in one spatial dimension over two Gaussian distributions, displaced from one another by a distance y. Since the three-dimensional Gaussian is nothing more than the product of three one-dimensional Gaussians, the convolution theorem immediately comes to our rescue and enables us to define the integral concentration overlap of puff p with that of puff m as:

$$\iiint_V \mathrm{c}_{jl}(\mathrm{t}) \cdot \mathrm{c}_{km}(\mathrm{t}) = \frac{(q_{jp}/\rho_p) \cdot (q_{km}/\rho_m)}{(2\pi)^{3/2} \cdot \sigma_{Tx} \cdot \sigma_{Ty} \cdot \sigma_{Tz}} \cdot \exp\left[-\frac{1}{2}\left(\frac{x^2}{\sigma_{Tx}^2} + \frac{y^2}{\sigma_{Ty}^2} + \frac{z^2}{\sigma_{Tz}^2} \right) \right] \qquad (21)$$

where q_{jp} is the mass of species j assigned to puff p, q_{km} is the species k mass of puff m; (x, y, z) specify the puff center separations; and the puff p-m overlap-sigma quantities σ_{Tx}, σ_{Ty}, and σ_{Tz} are given as:

$$\sigma^2_{Tx} = \sigma^2_{px} + \sigma^2_{mx} \,,\ \sigma^2_{Ty} = \sigma^2_{py} + \sigma^2_{my} \,, \text{ and } \sigma^2_{Tz} = \sigma^2_{pz} + \sigma^2_{mz} \,, \text{ respectively.}$$

In practice, the computational tedium of computing many thousands of Gaussians often leads developers to use simpler functions, such as the Epanechnikov kernel estimator (Epanechnikov, 1969) rather than the Gaussian. Like the Gaussian, such a 3-d kernel defines a spatially-diffuse concentration as:

$$\mathrm{c}_{jp} = \frac{(q_{jp}/\rho_p)}{\lambda_{px} \cdot \lambda_{py} \cdot \lambda_{pz}} \cdot f\left(\left| \frac{x'}{\lambda_{px}} \right| \right) \cdot f\left(\left| \frac{y'}{\lambda_{py}} \right| \right) \cdot f\left(\left| \frac{z'}{\lambda_{pz}} \right| \right) \qquad (22a)$$

where each "bandwidth" λ_p can be related to the corresponding σ_p, (e.g., the relation $\lambda_p = 2.214 \cdot \sigma_p$) and the function $f(\phi)$ is defined as:

$$f(\phi) = \begin{cases} \frac{3}{4}(1-\phi^2) & |\phi| \le 1 \\ 0 & |\phi| > 1 \end{cases} \quad \text{, where, for example, } \phi = |x'/\lambda|. \qquad (22b)$$

Another advantage of such a finite function which cuts off sharply for $|\phi| > 1$ (e.g., for $|x'/\lambda_{px}| > 1$) is that one has a very clear search window to look for neighboring puffs where the overlap integral is non-zero.

Once all the dm_i/dt quantities are determined, there is the bookkeeping issue of how to assign the mass change dm_i in species i back to the most-appropriate puffs in some proportionate way and without creating nasty problems, such as negative species mass being assigned to any puff/particle. This mass reassignment issue is discussed in Monforti et al. (2006).

3 Gaussian Regulatory Model Improvements

This section will consider recent improvements to U.S. EPA regulatory models that involve changes to the basic way in which the Gaussian solution is applied. Interestingly, some of these changes generally do not involve abandoning the Gaussian, but rather using more of them.

Our first example involves the case of dispersion under convective conditions. AERMOD (U.S. EPA, 2004 and Cimorelli et al., 2005) now treats such convective dispersion by employing two Gaussians: one whose centerline is advected upward by an updraft velocity and another whose centerline is advected downward by a downdraft velocity. These two Gaussians are weighted in proportion to the fractional area of updraft and downdraft zones, respectively. This formulation, developed by Weil and Brower (1984) and Weil (1985), results in asymmetric vertical dispersion that is in better agreement with the Willis and Deardorff (1978) water tank data than that which a single Gaussian could provide, but is completely consistent with the Gaussian approach.

A similar example that appears in AERMOD involves the treatment of flow over complex terrain, in that the final plume is a weighted sum of a plume, which follows terrain and one that does not.

A final AERMOD example involves the treatment of low wind speed conditions. As mentioned by Venkatram and Thé, (2003 - in Chapter 7A,Vol. 1), this issue of providing a proper azimuthal distribution as the mean wind goes is zero is bridged by using the weighted sum of a Gaussian distribution in y and a uniform azimuthal distribution and is given as:

$$H(x,y) = f_r \cdot \frac{1}{2 \cdot \pi \cdot r} + (1 - f_r) \cdot \frac{1}{\sqrt{2 \cdot \pi} \cdot \sigma_y} \exp\left(-\frac{y^2}{2 \cdot \sigma_y^2} \right) \tag{23}$$

where $f_r = \frac{2 \cdot \sigma_v^2}{U_e^2}$, $U_e \equiv \left(2 \cdot \sigma_v^2 + U_m^2 \right)^{1/2}$, U_m is the vector mean wind speed, and U_e provides the estimate of the total dilutionary wind.

Unfortunately, even this adjustment does not solve the problem of model over-prediction at very low wind speeds. Paine et al. (2010) reported over-predictions by a factor of 2-3 found in several low wind tracer studies, and have found it necessary to use a reformulated expression for the friction velocity, u^*, within the AERMET preprocessor to provide higher u^* at low mean winds, which in turn results in higher levels of vertical and horizontal turbulence and dilutionary wind U_e. Their analysis also suggested the need for imposing a minimum value of 0.4 m/s on σ_v.

For assessments involving mesoscale and longer-range transport (i.e., > 50 km.), CALMET (Scire et al., 1998) and CALPUFF (Scire et al., 2000; Scire, 2008) continues to be EPA's recommended Guideline modeling system; however, the more routine availability of high-resolution prognostic meteorological modeling has called into question some of CALMET's technical options (U.S. EPA et al, 2009) and the wisdom, in general, of filtering self-consistent, prognostic meteorological fields through a diagnostic wind field model with some historical shortcomings (e.g., divergence minimization ignoring air density, formulation in terrain-subtracted coordinates). As an alternative, more direct interface routines between the MM-5 and WRF models and CALPUFF are now being developed (Scire, 2008; Emery et al., 2009). Such more direct interfacing of high-quality meteorological fields, should improve the performance of CALPUFF in mesoscale and long-range tracer study comparisons (e.g., CAPTEX, ETEX) versus its performance using CALMET fields (Anderson and Brode, 2010).

It should also be noted that the wider and more routine availability of high-quality prognostic modeling results incorporating meteorological data assimilation, leads one to question the traditional regulatory dividing line of 50 km between using plume models and puff or particle models. A typical near-surface wind of 5 m/s only carries pollutants 18 km in one hour, and there are often terrain and intervening surface/land-use variations that challenge the assumptions of straight-line flows and uniform turbulence conditions. Low wind speeds represent yet another challenge to traditional plume modeling. Even if one relinquishes the need for specific hour-by-hour predictive power and requires only information about the highest concentration hours within a year or multi-year period, the presence of an intervening land-use shift between source and receptor (e.g., a large lake) could lead to systematic over-/under-predictions.

The CALPUFF model was designed to provide concentration predictions identical to the ISC-3 short-term dispersion model under the assumption of steady-state, uniform flow conditions, and could easily be modified to incorporate the dispersion modeling differences brought about by the transition from ISC to AERMOD (e.g., more realistic treatment of convective conditions), as anything that can be done with plumes can also be done with puffs or slugs (i.e., time-integrated puffs). Puff and particle models also incorporate along-wind dispersion, so that low or calm winds are not problematic.

The traditional objections to switching to puff or particle models, such as computational cost or requisite data base complexity become less relevant each year; however, there are major obstacles that science cannot circumvent, and these appear to arise (i.e., from a modelers perspective) from legal considerarions (e.g., precedence, the standing of existing air quality permits, resolution of discrepancies). These same non-scientific considerations also appear to have inhibited regulatory recognition and utilization of uncertainty estimates that arise from predictions of higher concentration moments (i.e., C^2 in addition to C -- as discussed in Section 2.1 and indirectly in Section 2.3). Regulators accepted photochemical grid modeling, not because it was a clever method but because it represented the only way to predict ozone and some secondary aerosol concentrations. A switch in the regulatory approach can only be anticipated when the current approach can be shown to be severely deficient on model performance grounds as opposed to being deficient merely on scientific principle grounds.

Acknowledgments

I would like to thank Professors Steven R. Hanna, Brian Sawford, and John D. Wilson and Dr. Joseph Chang, Gary Moore, and David Strimaitis for their useful comments. I would also like to acknowledge Mr. Robert Paine's providing me with recent AERMOD development manuscripts and helpful comments.

References

Anderson, B. A. and R. W. Brode, 2010. Evaluation of Four Lagrangian Models Against the Cross-Appalachian and European Tracer Experiments. Presented at the EPA Modeling Workshop, May 13, Portland, OR.

Bianconi, R., Mosca, S., and Graziani, G., 1999. PDM: a Lagrangian Particle Model for Atmospheric Dispersion. European Communities report 17721 EN, Ispra, Italy.

Cimorelli, A.J., S.G. Perry, A. Venkatram, J.C. Weil, R.J. Paine, R.B. Wilson, R.F. Lee, W.D. Peters, and R.W. Brode, 2005. AERMOD: A Dispersion Model for Industrial Source Applications. Part I: General Model Formulation and Boundary Layer Characterization. *J. Appl.Met.*, **44,** 682-693. American Meteorological Society, Boston, MA.

de Haan, P., 1999. On the use of density kernels for concentration estimations within particle and puff dispersion models. *Atmos. Environ.*, **33**, 2007-2021.

Doering, C, R. Akber, H. Heijnis, 2006. Vertical distributions of ^{210}Pb excess, ^{7}Be and ^{137}Cs in selected grass covered soils in Southeast Queensland, Australia. *J. Environ. Radioact.*, **87**, 135-147.

Durbin, P.A., 1983. Stochastic Differential Equations and Turbulent Dispersion, NASA Reference Publication 1103, NASA Lewis Research Center, Cleveland, OH, 73pp.

Emery, C., B. Brashers, and B. Anderson, 2009. A New Direct MM5/WRF Meteorological Interface Program for CALPUFF. Presented at the AWMA Guideline on Air Quality Models: Next Generation of Models, Oct. 28, Raleigh, NC.

Epanechnikov, V.K., 1969. Non-parametric estimation of a multivariate probability density. Theory of Probability and its Applications, **14**, 153-158.

Carslaw, H.S. and J.C. Jaeger, 1959. *Conduction of Heat in Solids*, Second Edition. Clarendon Press, Oxford.

Drivas, P.J., T.S. Bowers, and R. J. Yamartino, 2010. Soil Mixing after Surface Deposition: I. Theory. *Environ. Sci. Technol*., submitted for publication.

Gifford, F. A., 1959: Statistical properties of a fluctuation plume dispersion model. *Advances in Geophysics,* **6**, 117–138.

Hanna, S. R., 1986: Spectra of concentration fluctuations: The two time scales of a meandering plume. *Atmos. Environ.,* **20,** 1131–1137.

Kaste, J. M., A. M. Heimsath, B. C. Bostick, 2007. Short-term soil mixing quantified with fallout radionuclides. *Geology*, **35**, 243-246.

Lemons, D. S., 2002. *An Introduction to Stochastic Processes in Physics*. The Johns Hopkins University Press, Baltimore, MD, 124 pp.

Luhar, A. K., R. E., Britter, 1989. A random walk model for dispersion in inhomogeneous turbulence in a convective boundary layer. *Atmos Environ*, **23**, 1911–1924.

Monforti, F., L. Vitali, G. Pagnini, R. Lorenzini, L. Delle Monache, and G. Zanini, 2006: Testing kernel density reconstruction for Lagrangian photochemical modelling. *Atmos. Environ.,* **40,** 7770-7785.

Paine, R. J., J. A. Connors, and C. D. Szembek, 2010: AERMOD Low Wind Speed Evaluation Study: Results and Implementation. AWMA Paper 2010-A-631-AWMA

Pope, S. B., 2000. *Turbulent Flows*. Cambridge University Press, UK, 806pp.

Rosen, K, I. Oborn, H. Lonsjo, 1999. Migration of radiocaesium in Swedish soil profiles after the Chernobyl accident, 1987-1995. *J. Environ. Radioact.*, **46**, 45-66.

Sawford, B. L., 1985: Concentration statistics for surface plumes in the atmospheric boundary layer. *Proc. Seventh Symp. on Turbulence and Diffusion,* Boulder, CO, pp. 323–326.

Sawford, B. L. and H. Stapountzis, 1986: Concentration fluctuations according to fluctuating plume models in one and two dimensions. *Bound.-Layer Meteor.,* **37,** 89–105.

Scire, J., 2008. Development, Maintenance and Evaluation of CALPUFF. Presented at the Ninth Conference on Air Quality Modeling, Oct. 9-10, Research Triangle Park, NC.

Scire, J.S., D.G. Strimaitis and R.J. Yamartino, 2000. User's guide for the CALPUFF dispersion model (Version 5). Earth Tech, Inc., Concord, MA.

Scire J.S., F.R. Robe, M.E. Fernau, and R.J. Yamartino, 1998. A User's Guide for the CALMET Meteorological Model (Version 5.0). Earth Tech, Inc., Concord, MA.

U.S. EPA, National Park Service, and U.S. Fish and Wildlife Service, 2009. Reassessment of the Interagency Workgroup on Air Quality Modeling (IWAQM) Phase 2 Summary Report: Revisions to Phase 2 Recommendations. DRAFT Report EPA-454/R-09-xxx.

U.S. EPA, 2004. AERMOD: Description of Model Formulation. EPA-454/R-03-004. Available from http://www.epa.gov/scram001 .

van Dop, H., F. T. M. Nieuwstadt, and J. C. R. Hunt, 1985. Random walk models for particle displacements in inhomogeneous unsteady turbulent flows. *Phys. Fluids*, **28**, 1639-1653.

Venkatram, A. and J. Thé, 2003. Introduction to Gaussian Plume Models. Chapter 7A in *Air Quality Modeling: Volume I – Fundamentals*. Paolo Zannetti, Ed., EnviroComp Institute and the Air and Waste Management Association.

Weil, J.C., and R. P. Brower, 1984. An updated Gaussian plume model for tall stacks. *J. Air Pollut. Control Assoc.,* **34**, 818–827.

Weil, J.C., 1985, Updating applied diffusion models. *J. Clim. App. Meteor.,* **24**(11), 1111-1130.

Willis, G. E. and J. W. Deardorff, 1978. A laboratory study of dispersion from elevated source within a modeled convection mixed layer. *Atm. Env.*, **12**, 1305-1311.

Wilson, J. D., 2007. Turbulent velocity distributions and implied trajectory models. Boundary-Layer Meteorol., **125**, 39–47.

Yamartino, R.J., 2008a. Gaussian Puff Modeling. Chapter 8A of *AIR QUALITY MODELING - Theories, Methodologies, Computational Techniques, and Available Databases and Software. Vol. III – Advanced Topics*. (P. Zannetti, Editor). Published by The EnviroComp Institute and the Air & Waste Management Association.

Yamartino, R.J., 2008b. Simulation Algorithms in Gaussian Plume Modeling. Chapter 7B of AIR QUALITY MODELING - Theories, Methodologies, Computational Techniques, and Available Databases and Software. Vol. III – Advanced Topics. (P. Zannetti, Editor). Published by The EnviroComp Institute and the Air & Waste Management Association.